Magnetoanisotropic Andreev Reflection in Ferromagnet-Superconductor Junctions

Petra Högl, Alex Matos-Abiague, Igor Žutić, and Jaroslav Fabian

Phys. Rev. Lett. **115**, 116601 — Published 10 September 2015

DOI: 10.1103/PhysRevLett.115.116601

Magnetoanisotropic Andreev Reflection in Ferromagnet/Superconductor Junctions

Petra Högl,[1] Alex Matos-Abiague,[1,2] Igor Žutić,[2] and Jaroslav Fabian[1]
[1] *Institute for Theoretical Physics, University of Regensburg, 93040 Regensburg, Germany*
[2] *Department of Physics, University at Buffalo, State University of New York, Buffalo, NY 14260, USA*
(Dated: June 24, 2015)

Andreev reflection spectroscopy of ferromagnet/superconductor (F/S) junctions is an important probe of spin polarization. We theoretically investigate spin-polarized transport in F/S junctions in the presence of Rashba and Dresselhaus interfacial spin-orbit fields and show that Andreev reflection can be controlled by changing the magnetization orientation. We predict a giant in- and out-of-plane magnetoanisotropy of the junction conductance. If the ferromagnet is highly spin polarized—in the half-metal limit—the magnetoanisotropic Andreev reflection depends universally on the spin-orbit fields only. Our results show that Andreev reflection spectroscopy can be used for sensitive probing of interfacial spin-orbit fields in F/S junction.

Spin-orbit coupling (SOC) is a key interaction in spintronics [1–3], allowing an electrical control of magnetization and, vice versa, a magnetic control of electrical current. In systems lacking space inversion symmetry—be it bulk, hybrid structures, junctions—SOC induces spin-orbit fields [1, 2] as an emergent phenomenon. We are in particular concerned here with interfacial spin-orbit fields which are believed to be behind a wealth of new phenomena, not existent or fragile in the bulk, such as the tunneling anisotropic magnetoresistance (TAMR) [4–7], interfacial spin-orbit torques [8], or skyrmions [9].

Interfacial spin-orbit fields are also important in semiconductor/superconductor [10–13] and F/S junctions [14] for creating Majorana quasiparticle states. It is the latter junctions that we focus on. We investigate the interplay of magnetism and spin-orbit fields. We show that this interplay leads to marked anisotropies in the junction conductance with respect to the orientation of magnetization. The most robust is the out-of-plane anisotropy (plane being the interface), which arises from the omnipresent Rashba field [15]. A more subtle is the in-plane anisotropy, which arises from the interference between the Rashba and Dresselhaus [16] fields, induced by a two-fold anisotropy of the C_{2v} type. A zinc-blende semiconductor (say, GaAs or InAs) as a barrier in an F/S junction would create such an anisotropy, generating spin-orbit fields C_{2v} "butterflies" patterns, as shown by first-principles calculations [17]. Remarkably, the resulting magnetoconductance anisotropy—we term it *magnetoanisotropic Andreev reflection (MAAR)*—is giant in comparison to TAMR, its normal-state counterpart, reaching a universal behavior in the half-metallic case. This is because Andreev reflection (AR) (which has no counterpart in the normal-state TAMR) is strongly influenced by interfacial spin-orbit fields.

We specifically examine the influence of SOC and crystalline anisotropy on the process of AR in which the reflected particle carries the information about both the phase of the incident particle and the macroscopic phase of the superconductor to which a Cooper pair is being transferred [18]. AR is thus responsible for the proximity effect in which the phase correlations are introduced to a nonsuperconducting material [19–23]. While the main interest in AR is currently the proximity effect coupled with SOC, inducing Majorana states, in spintronics AR is used to probe the spin polarization in F/S junctions [18–34]. We argue that AR can also be a sensitive probe of interfacial spin-orbit fields.

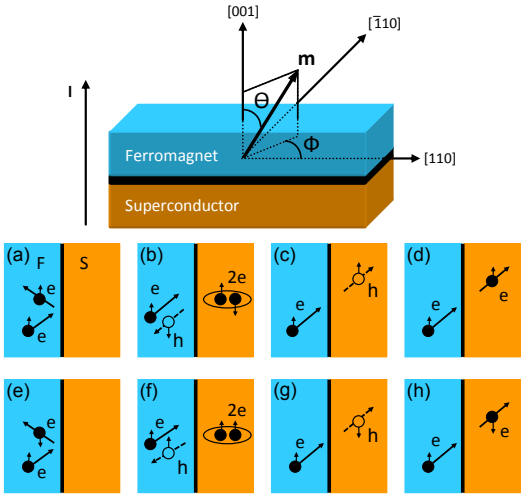

FIG. 1. (Color online) Top: F/S junction. Magnetization vector $\boldsymbol{m}$ is given by the polar angle Θ and azimuthal angle Φ. Current, I, flows perpendicular to the interface. To specify spin-orbit fields we use principal crystallographic orientations $x = [110]$, $y = [\bar{1}10]$, and $z = [001]$. Bottom: Scattering processes at the F/S interface with SOC. Electrons (holes) are depicted by full (empty) circles. Vertical arrows denote the spin. The processes for a spin up incoming electron: (a) Specular reflection, (b) Andreev reflection, (c) hole-like transmission, and (d) electron-like transmission. (e)-(h) Corresponding spin-flip counterparts. Spin-flip (equal electron and hole spins) Andreev reflection is in (f).

Our model F/S junction consists of F ($z < 0$) and S ($z > 0$) semi-infinite regions separated by a flat interface at $z = 0$, with potential and SOC scattering. The scheme and possible scattering channels are illustrated in Fig. 1. For example, in conventional AR the incoming electron

is reflected as a hole with the opposite spin, while spin-flip AR implies equal spin of the incoming and reflected particles. These two AR processes, see Figs. 1(b) and (f), introduce, respectively spin-singlet and spin-triplet superconducting correlations at the interface [22, 23].

We consider epitaxial-quality junctions, such as those used in TAMR [6], or point contact geometries [35], in which ballistic transport formalism is applicable. In diffusive tunnel junctions AR could be enhanced by electron-hole coherence [36]. In ferromagnetic junctions such effects would be absent for normal AR due to short coherence length, but spin-flip AR could be enhanced. (Ordinary effects of diffusion could be accounted for by renormalizing the tunneling parameters [32]). We generalize the BTK formalism [37] and solve the Bogoliubov-de Gennes equation [38] for quasiparticle states $\Psi(\mathbf{r})$ with energy E,

$$\begin{pmatrix} \hat{H}_e & \hat{\Delta} \\ \hat{\Delta}^\dagger & \hat{H}_h \end{pmatrix} \Psi(\mathbf{r}) = E\Psi(\mathbf{r}), \tag{1}$$

with the single-particle Hamiltonian for electrons $\hat{H}_e = -(\hbar^2/2)\boldsymbol{\nabla}[1/m(z)]\,\boldsymbol{\nabla} - \mu(z) - (\Delta_{xc}/2)\Theta(-z)\mathbf{m}\cdot\hat{\boldsymbol{\sigma}} + \hat{H}_B$; for holes $\hat{H}_h = -\hat{\sigma}_y \hat{H}_e^* \hat{\sigma}_y$. The unit magnetization vector (see Fig. 1) is $\mathbf{m} = [\sin\Theta\cos\Phi, \sin\Theta\sin\Phi, \cos\Theta]$, $\hat{\boldsymbol{\sigma}}$ are Pauli matrices, Δ_{xc} is the exchange spin splitting in the F region (Stoner model), $m(z)$ is the effective mass, and $\mu(z)$ is the chemical potential. The interfacial scattering is modeled as $\hat{H}_B = (V_0 d + \mathbf{w}\cdot\hat{\boldsymbol{\sigma}})\,\delta(z)$, where V_0 and d are the barrier height and width, while $\mathbf{w} = [(\alpha-\beta)k_y, -(\alpha+\beta)k_x, 0]$ is the effective SOC field including Rashba and Dresselhaus terms [1, 2], parametrized by α and β, respectively, for the crystallographic orientations see Fig. 1. The superconducting pair potential is given by $\hat{\Delta} = \Delta\Theta(z)\mathbb{1}_{2\times 2}$ (the accuracy of such a step-function form of $\hat{\Delta}$ is discussed in [39]), with the isotropic gap Δ. Similar methodology, for half-metal/S junctions with Rashba coupling inside the superconductor was employed in Ref. [40]. With Rashba-only SOC one should still obtain out-of-plane magnetoanisotropy, and this is already implicit in this formalism [40].

Since the in-plane wave vector $\mathbf{k}_{||}$ is conserved, $\Psi_\sigma(\mathbf{r}) = \Psi_\sigma(z)e^{i\mathbf{k}_{||}\mathbf{r}_{||}}$. The solution in the F region for incoming electrons with spin σ is

$$\Psi_\sigma^F = \frac{1}{\sqrt{k_\sigma^e}} e^{ik_\sigma^e z}\chi_\sigma^e + r_{\sigma,\sigma}^e e^{-ik_\sigma^e z}\chi_\sigma^e + r_{\sigma,-\sigma}^e e^{-ik_{-\sigma}^e z}\chi_{-\sigma}^e + r_{\sigma,-\sigma}^h e^{ik_{-\sigma}^h z}\chi_{-\sigma}^h + r_{\sigma,\sigma}^h e^{ik_\sigma^h z}\chi_\sigma^h, \tag{2}$$

with the spinors for the electron-like $\chi_\sigma^e = (\chi_\sigma, 0)^T$ and hole-like $\chi_\sigma^h = (0, \chi_{-\sigma})^T$ quasiparticles, both containing

$$\chi_\sigma^T = \left(\sigma\sqrt{1+\sigma\cos\Theta}e^{-i\Phi}, \sqrt{1-\sigma\cos\Theta}\right)/\sqrt{2}, \tag{3}$$

where $\sigma = 1(-1)$ corresponds to the spin parallel (antiparallel) to $\hat{\mathbf{m}}$. The electron-like (hole-like) quasiparticle wave vectors in the F region are $k_\sigma^{e(h)} = \sqrt{k_F^2 + 2m_F/\hbar^2\,[(-)E + \sigma\Delta_{xc}/2] - k_{||}^2}$.

In the S region the scattering states are

$$\Psi_\sigma^S = t_{\sigma,\sigma}^e e^{iq^e z}\begin{pmatrix} u \\ 0 \\ v \\ 0 \end{pmatrix} + t_{\sigma,-\sigma}^e e^{iq^e z}\begin{pmatrix} 0 \\ u \\ 0 \\ v \end{pmatrix} + t_{\sigma,\sigma}^h e^{-iq^h z}\begin{pmatrix} v \\ 0 \\ u \\ 0 \end{pmatrix} + t_{\sigma,-\sigma}^h e^{-iq^h z}\begin{pmatrix} 0 \\ v \\ 0 \\ u \end{pmatrix}, \tag{4}$$

where the quasiparticle wave vectors are given by $q^{e(h)} = \sqrt{q_F^2 + (-)2m_S/\hbar^2\sqrt{E^2-\Delta^2} - k_{||}^2}$. The superconducting coherence factors satisfy $u^2 = 1 - v^2 = \left(1 + \sqrt{E^2-\Delta^2}/E\right)/2$.

Using charge current conservation, the differential conductance at zero temperature, normalized by the Sharvin conductance [1] $G_{Sh} = e^2 k_F^2 A/(2\pi h)$ of a perfect contact, is

$$G = \sum_\sigma \int \frac{d^2\mathbf{k}_\parallel}{2\pi k_F^2}\left[1 + R_\sigma^h(-e\mathrm{V}) - R_\sigma^e(e\mathrm{V})\right], \tag{5}$$

containing the probability amplitudes in the F region $R_\sigma^{e(h)}(E, \mathbf{k}_\parallel) = \mathrm{Re}\left(k_\sigma^{e(h)}\left|r_{\sigma,\sigma}^{e(h)}\right|^2 + k_{-\sigma}^{e(h)}\left|r_{\sigma,-\sigma}^{e(h)}\right|^2\right)$ which combine the coefficients for the scattering processes with and without spin flip for specular and AR; V is the bias voltage and A is the interfacial area.

To describe our results we introduce dimensionless quantities: $Z = V_0 d\sqrt{m_F m_S}/\left(\hbar^2\sqrt{k_F q_F}\right)$ denotes the barrier strength [31, 37], $\lambda_\alpha = 2\alpha\sqrt{m_F m_S}/\hbar^2$ and $\lambda_\beta = 2\beta\sqrt{m_F m_S}/\hbar^2$ quantify the Rashba and Dresselhaus SOC, and $P = (\Delta_{xc}/2)/\mu_F$ defines the spin polarization in F.

We first examine the influence of SOC on the F/S conductance (see Fig. 2), for a metallic point contact ($Z = 0$) and for a moderate barrier ($Z = 1$). For the former case the conductance tends to decrease with increasing SOC. Even in the half-metallic case ($P = 1$) SOC does not give a finite subgap conductance; spin-flip AR is suppressed. In contrast, for moderate barrier ($Z = 1$), SOC enhances the conductance due to spin-flip AR, even for $P = 1$. Interestingly, at eV $= \Delta$ the conductance is not affected by SOC for any Z. Focusing on $G(0)$, Fig. 2 shows that in a metallic contact increasing SOC steadily reduces $G(0)$, while for a moderate barrier $G(0)$ is a non-monotonic function of SOC, with a (P-dependent) maximum which turns out to be due to spin-flip AR.

The absence of spin-flip AR in metallic contacts can be explained analytically. For eV $\leq \Delta$ quasiparticle transmission is prohibited and subgap conductance $G \sim \sum_\sigma \int d^2\mathbf{k}_\parallel\, 2R_\sigma^h(-e\mathrm{V})$. In the half-metallic case the only contribution to AR comes from spin-flip AR,

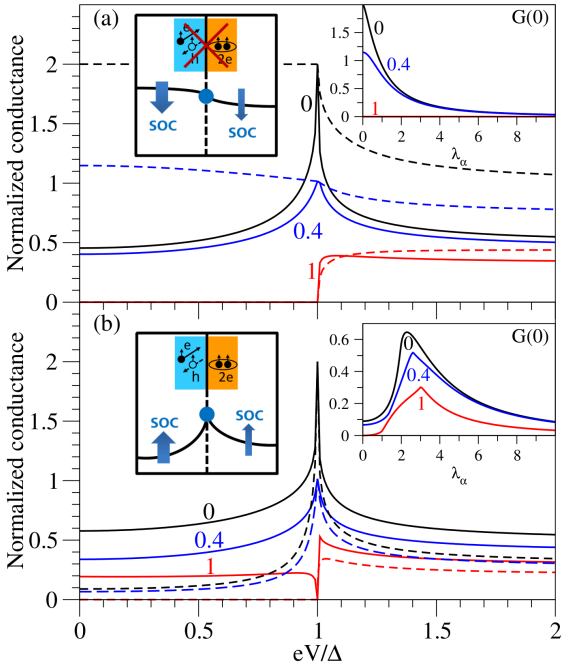

FIG. 2. (Color online) Calculated normalized conductance, $G(eV/\Delta)$, for different (indicated) spin polarizations P. Rashba SOC is $\lambda_\alpha = 2$ and Dresselhaus SOC is $\lambda_\beta = 0$. Magnetization is in-plane ($\Theta = \pi/2$). (a) No interfacial barrier ($Z = 0$), and (b) modest interfacial barrier ($Z = 1$) cases are shown. The dashed lines show G without SOC. The insets show the dependence of $G(0)$ on Rashba SOC. In (a), the subgap conductance for $P = 1$ vanishes for every $\lambda_{\alpha,\beta}$; in the inset $G(0) = 0$ for this case. The illustrations summarize main qualitative impacts of SOC on conductance.

$R^h_\sigma(E) = \mathrm{Re}\left(k^h_\sigma \left|r^h_{\sigma,\sigma}\right|^2\right)$, because of the missing minority spin subband in F. To lowest order in SOC and Z then $G(0) \propto Z^2\lambda_i^2$ with $i \in \{\alpha, \beta\}$ [41], vanishing if $Z = 0$. This perturbative quadratic dependence on the spin-orbit strength was also obtained in Ref. [40].

The calculated conductance features of SOC [42–46] can be distinguished from *k-independent* spin-flip scattering by magnetic moments: For $Z = 0$ SOC always reduces the conductance and the subgap conductance vanishes for $P = 1$. In contrast, k-independent spin-flip scattering [47] can increase the conductance and the subgap conductance is in general finite for $P = 1$. However, similar features as those of SOC can arise in exotic superconductors without bulk inversion symmetry [48].

While the conductance changes are indicative of interfacial SOC, magnetic anisotropy of the conductance is a true fingerprint. As the main contribution comes from AR, we call this anisotropy effect *magnetoanisotropic Andreev reflection*. We consider two configurations: in-plane, in which magnetization $\mathbf{m}$ changes azimuthally (Φ) in the interfacial plane, and out-of-plane, with polar (Θ) changes of $\mathbf{m}$ in a perpendicular plane (see Fig. 1).

We define the in-plane MAAR as

$$\mathrm{MAAR}_{[110]}(\Phi) = \left.\frac{G(\Theta,0) - G(\Theta,\Phi)}{G(\Theta,\Phi)}\right|_{\Theta=90^\circ}, \quad (6)$$

and the out-of-plane MAAR as

$$\mathrm{MAAR}_{[1\bar{1}0]}(\Theta) = \left.\frac{G(0,\Phi) - G(\Theta,\Phi)}{G(\Theta,\Phi)}\right|_{\Phi=-90^\circ}. \quad (7)$$

The out-of-plane MAAR depends, in general on Φ, but we choose the yz ($\Phi = -90^\circ$) plane as its reference.

The calculated MAAR, in Fig. 3, shows a nonmonotonic dependence on SOC. For metallic contacts ($Z = 0$) MAAR is determined by the magnetoanisotropy of conventional AR. In the presence of a barrier (exemplified by $Z = 1$), MAAR gets strongly enhanced due to the additional contribution from spin-flip AR. In-plane MAAR exhibits C_{2v} symmetry due to the interplay of Rashba and Dresselhaus fields, similarly to TAMR [2, 6, 7]. If either of the two fields is absent, in-plane MAAR vanishes. In contrast, out-of-plane MAAR is finite even with the Rashba field alone, which makes it a robust probe of this important interfacial SOC. Interestingly, at eV = Δ MAAR is always absent, as there are no effects of SOC

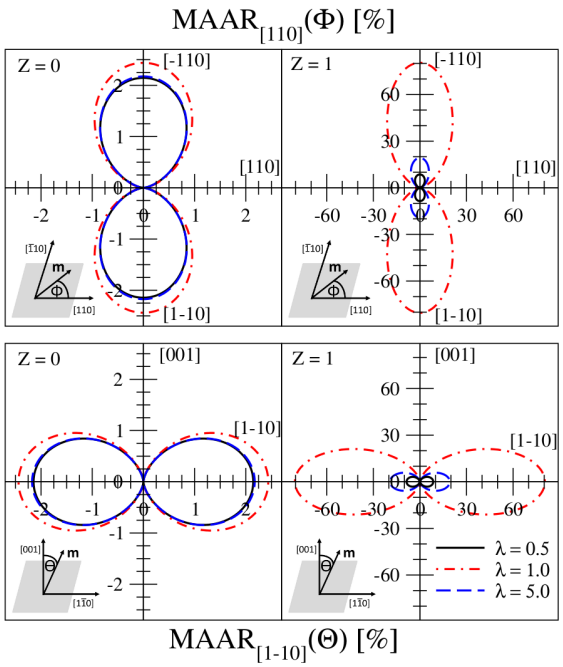

FIG. 3. (Color online) Top: Calculated in-plane magnetoanisotropic Andreev reflection (MAAR) with [110] crystallographic reference axis for $Z = 0$ (left) and $Z = 1$ (right) for different strengths of SOC $\lambda_\alpha = \lambda_\beta = \lambda$ at $P = 0.4$ and $V = 0$. Bottom: Out-of-plane MAAR with $[1\bar{1}0]$ crystallographic reference axis. For $Z = 0$ the lines of $\lambda = 0.5$ and $\lambda = 5.0$ coincide. For the chosen reference axes and $\lambda_\alpha = \lambda_\beta$ the in-plane and out-of-plane MAAR curves have the same magnitude and shape, but rotated to the corresponding reference axis.

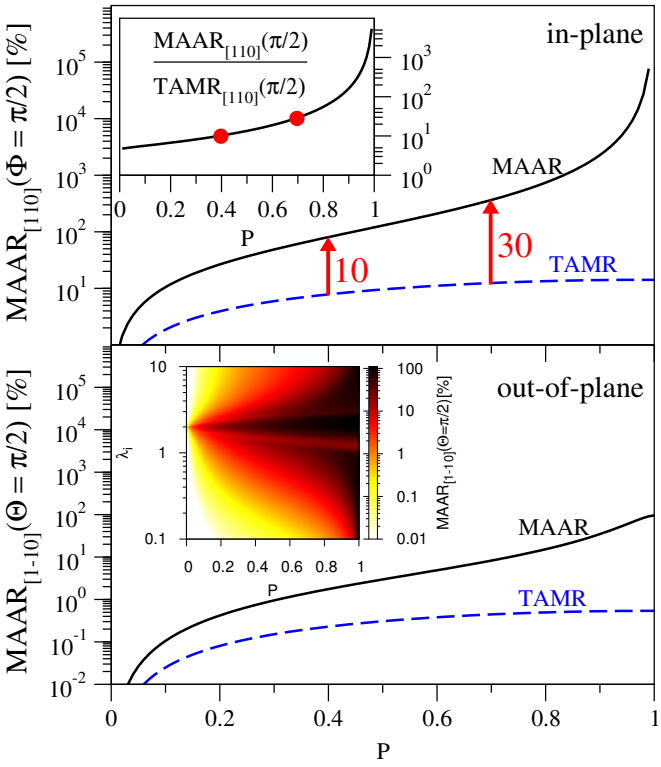

FIG. 4. (Color online) Calculated in-plane (top) and out-of-plane (bottom) MAAR and TAMR as a function of spin polarization P for a moderate barrier ($Z = 1$) and $V = 0$. The in-plane case is calculated with $\lambda_\alpha = \lambda_\beta = 1$, while for out-of-plane we have included Rashba $\lambda_\alpha = 0.5$ only. The top inset shows the ratio of MAAR and TAMR for the in-plane case, while the bottom inset shows the color map of out-of-plane MAAR as a function of P and Rashba (or Dresselhaus) SOC λ_i (where i could be either α or β).

on G here; see the discussion to Fig. 2. Additional effects (such as appearance of symmetry lobes) can arise due to the effective mass and Fermi wave vector mismatch [41].

Compared to TAMR, the magnitude of MAAR is giant, varying by orders of magnitude upon changing the spin polarization P. (The experimentally measured in-plane TAMR in Fe/GaAs/Au junctions is less than a percent [6].) A detailed model comparison is shown in Fig. 4 for both in- and out-of-plane configurations; TAMR is evaluated by setting $\Delta = 0$. For a typical P of 40%, the ratio MAAR/TAMR is about 10. Moving towards half metals ($P \gtrsim 80\%$), this ratio climbs to more than 10^2! This giant increase is best illustrated in the half-metallic limit of $P = 1$. For a weak SOC (which is typically the case) an analytical treatment gives [41],

$$\mathrm{MAAR}_{[110]}(\Phi) \approx \frac{2\lambda_\alpha\lambda_\beta(1-\cos 2\Phi)}{\lambda_\alpha^2+\lambda_\beta^2+2\lambda_\alpha\lambda_\beta\cos 2\Phi}, \qquad (8)$$

$$\mathrm{MAAR}_{[1\bar{1}0]}(\Theta) \approx \frac{(\lambda_\alpha+\lambda_\beta)^2(1-\cos 2\Theta)}{3(\lambda_\alpha^2+\lambda_\beta^2)-2\lambda_\alpha\lambda_\beta+(\lambda_\alpha+\lambda_\beta)^2\cos 2\Theta}. \qquad (9)$$

Therefore, the in-plane $\mathrm{MAAR}_{[110]}(\Phi = \pi/2) \approx 4\lambda_\alpha\lambda_\beta/(\lambda_\alpha - \lambda_\beta)^2$, and out-of-plane $\mathrm{MAAR}_{[1\bar{1}0]}(\Theta = \pi/2) \approx (\lambda_\alpha + \lambda_\beta)^2/(\lambda_\alpha - \lambda_\beta)^2$, *depending universally on the spin-orbit fields only*, and *diverging* as $\lambda_\alpha \approx \lambda_\beta$ (see the in-plane case in Fig. 4). In contrast, TAMR, which is proportional to the product $\lambda_\alpha\lambda_\beta$ [7], has no singular behavior, and is not a universal function of λ_i only.

We can trace this giant enhancement of MAAR over TAMR to spin-flip AR. Let us separate phenomenologically the conductance $G = G^{(0)} + G_{so}$ into the sum of SOC independent and dependent parts. In TAMR typically $G^{(0)} \gg G_{so}$, and TAMR $\sim G_{so}/G^{(0)} \ll 1$, even for $P \approx 1$. But in F/S junctions $G^{(0)}$ decreases with increasing P, eventually vanishing in the half-metallic limit. For $P \approx 1$ the conductance of the F/S junction is dominated by the spin-flip AR contribution to G_{so}. Thus, SOC determines both the conductivity and the magnetoanisotropy. Furthermore, if $\lambda_\alpha \approx \pm\lambda_\beta$, the spin-flip AR, and so the conductance, can be switched *on* and *off* by changing the orientation of $\mathbf{m}$. For $\lambda_\alpha = \lambda_\beta$ and $\Phi = 0$, $\mathbf{m} \perp \mathbf{w}$ and spin-flip AR yields a finite G. However, if $\Phi = \pi/2$, then $\mathbf{m} \parallel \mathbf{w}$ and spin-flip processes are strongly suppressed; $G(eV \le \Delta)$ at $\Phi = \pi/2$ vanishes. As a result, *in-plane MAAR diverges if* $\lambda_\alpha = \lambda_\beta$. Similarly for out-of-plane MAAR.

There is one more peculiarity of MAAR in the half-metallic limit. If only Rashba (or only Dresselhaus) SOC is present, MAAR has a *fixed universal* magnitude of 100%. This case is shown for the out-of-plane configuration in Fig. 4 (in particular the inset for $\lambda_i \lesssim 1$ shows MAAR of 100% for $P \approx 1$). It follows from Eq. (9) that $\mathrm{MAAR}_{[1\bar{1}0]}(\Theta) \approx (1-\cos 2\Theta)/(3+\cos 2\Theta)$, which gives a universal amplitude of 100% for $\Theta = \pi/2$. In other words, $G(\Theta = 0) = 2G(\Theta = \pi/2)$. The origin of this universal behavior is traced to the spin-flip probability by scattering of spin-polarized electrons off spin-orbit fields. The conductance is determined by spin-flip AR. For out-of-plane magnetization, $\Theta = 0$, two fields, one along x and one along y, induce a spin flip. But for an in-plane magnetization, say along x, $\Theta = \pi/2$, only the spin-orbit field component along y can flip the spin. This gives the 2:1 ratio in conductances and 100% of MAAR. A more technical and detailed discussion of the differences between MAAR and TAMR can be found in Ref. 41.

Experimental realization of MAAR could follow the measurement geometry of TAMR [6], ideally also the same junction, with the nonmagnetic metal that becomes superconducting at low temperatures. Magnetization of the ferromagnetic layer is typically rotated by an external magnetic field. This field can bring additional anisotropic orbital effects whose presence can be clearly identified from the field magnitude dependence [49]. However, one can avoid these extrinsic effects entirely if one uses dysprosium magnets which can be oriented by the field, but do not need its presence to remain in the rotated posi-

tion [50]. Potential aspects of non-flat tunneling barriers can also be treated [51]. A practical alternative (especially if ballistic junctions are desired) could be a point contact F/S junction geometry [35, 52].

To conclude, we have applied a well established theoretical formalism to systematically explore the magnetic anisotropy of the conductance in F/S junctions due to interfacial SOC. We predict a giant in- and out-of-plane MAAR—when compared with TAMR—exhibiting universal characteristics in the half-metallic regime. The predicted magnetization control of the AR suggests a similar control of the superconducting proximity effect and Majorana states. Our findings reveal an unexplored venue for AR spectroscopy, in the sensitive probing of interfacial SOC and related magnetoanisotropic phenomena.

We acknowledge useful discussions with D. Weiss, C. Strunk, C. Back, B. Nadgorny, and P. Stamenov. This work has been supported by the DFG SFB 689, International Doctorate Program Topological Insulators of the Elite Network of Bavaria, DOE-BES Grant DE-SC0004890 (I.Z.), and ONR N000141310754 (A.M.).

[1] I. Žutić, J. Fabian, and S. Das Sarma, Rev. Mod. Phys. **76**, 323 (2004).
[2] J. Fabian, A. Matos-Abiague, C. Ertler, P. Stano, and I. Žutić, Acta Phys. Slov. **57**, 565 (2007).
[3] S. Maekawa, *Concepts in Spin Electronics* (Oxford University Press, Oxford, 2006).
[4] L. Brey, C. Tejedor, and J. Fernandez-Rossier, Appl. Phys. Lett. **85**, 1996 (2004).
[5] C. Gould, C. Rüster, T. Jungwirth, E. Girgis, G. M. Schott, R. Giraud, K. Brunner, G. Schmidt, and L. W. Molenkamp, Phys. Rev. Lett. **93**, 117203 (2004).
[6] J. Moser, A. Matos-Abiague, D. Schuh, W. Wegscheider, J. Fabian, and D. Weiss, Phys. Rev. Lett. **99**, 056601 (2007).
[7] A. Matos-Abiague and J. Fabian, Phys. Rev. B **79**, 155303 (2009); A. Matos-Abiague, M. Gmitra, and J. Fabian, *ibid.* **80**, 045312 (2009).
[8] K. S. Ryu, L. Thomas, S. H. Yang, and S. Parkin, Nanotech. **8**, 527 (2013); A. Chernyshov, M. Overby, X. Liu, J. K. Furdyna, Y. Lyanda-Geller, and L. P. Rokhinson, Nature Phys. **5**, 656 (2009).
[9] A. Fert, V. Cros, and J. Sampaio, Nature Nanotech. **8**, 152 (2013).
[10] R. M. Lutchyn, J. D. Sau, and S. Das Sarma, Phys. Rev. Lett. **105**, 077001 (2010).
[11] Y. Oreg, G. Refael, and F. von Oppen, Phys. Rev. Lett. **105**, 177002 (2010).
[12] V. Mourik, K. Zuo, S. M. Frolov, S. R. Plissard, E. P. A. M. Bakkers, and L. P. Kouwenhoven, Science **336**, 1003 (2012).
[13] L. P. Rokhinson, X. Liu, and J. K. Furdyna, Nature Phys. **8**, 795 (2012).
[14] S. Nadj-Perge, I. K. Drozdov, J. Li, H. Chen, S. Jeon, J. Seo, A. H. MacDonald, B. A. Bernevig, and A. Yazdani, Science **346**, 6209 (2014).
[15] Y. A. Bychkov and E. I. Rashba, J. Phys. C **17**, 6039 (1984).
[16] G. Dresselhaus, Phys. Rev. **100**, 580 (1955).
[17] M. Gmitra, A. Matos-Abiague, C. Draxl, and J. Fabian, Phys. Rev. Lett. **111**, 036603 (2013).
[18] G. Deutscher, Rev. Mod. Phys. **77**, 109 (2005).
[19] A. I. Buzdin, Rev. Mod. Phys. **77**, 935 (2005).
[20] F. S. Bergeret, A. F. Volkov, and K. B. Efetov, Rev. Mod. Phys. **77**, 1321 (2005).
[21] A. A. Golubov, M. Y. Kupriyanov, and E. Il'ichev, Rev. Mod. Phys. **76**, 411 (2004).
[22] M. Eschrig, Phys. Today **64**, 43 (2011).
[23] C. Visani, Z. Sefrioui, J. Tornos, C. Leon, J. Briatico, M. Bibes, A. Barthélémy, J. Santamaría, and J. E. Villegas, Nature Phys. **8**, 539 (2012).
[24] S. Kashiwaya and Y. Tanaka, Rep. Prog. Phys. **63**, 1641 (2000).
[25] M. J. M. de Jong and C. W. J. Beenakker, Phys. Rev. Lett. **74**, 1657 (1995).
[26] R. J. Soulen, J. M. Byers, M. S. Osofsky, B. Nadgorny, T. Ambrose, S. F. Cheng, P. R. Broussard, C. T. Tanaka, J. Nowak, J. S. Moodera, A. Barry, and J. M. D. Coey, Science **282**, 85 (1998).
[27] S. K. Upadhyay, A. Palanisami, R. N. Louie, and R. A. Buhrman, Phys. Rev. Lett. **81**, 3247 (1998).
[28] J. X. Zhu, B. Friedman, and C. S. Ting, Phys. Rev. B **59**, 9558 (1999).
[29] S. Kashiwaya, Y. Tanaka, N. Yoshida, and M. R. Beasley, Phys. Rev. B **60**, 3572 (1999).
[30] I. Žutić and S. Das Sarma, Phys. Rev. B **60**, R16322 (1999).
[31] I. Žutić and O. T. Valls, Phys. Rev. B **60**, 6320 (1999); **61**, 1555 (2000).
[32] I. I. Mazin, A. A. Golubov, and B. Nadgorny, J. Appl. Phys. **89**, 7576 (2001).
[33] K. Kikuchi, H. Imamura, S. Takahashi, and S. Maekawa, Phys. Rev. B **65**, 020508 (2001).
[34] C. S. Turel, I. J. Guilaran, P. Xiong, and J. Y. T. Wei, Appl. Phys. Lett. **99**, 192508 (2011).
[35] P. Stamenov, J. Appl. Phys **111**, 07C519 (2012); **113**, 17C718 (2013).
[36] F. W. J. Hekking and Y. V. Nazarov, Phys. Rev. Lett. **71**, 1625 (1993).
[37] G. E. Blonder, M. Tinkham, and T. M. Klapwijk, Phys. Rev. B **25**, 4515 (1982).
[38] P. G. De Gennes, *Superconductivity of metals and alloys* (Addison-Wesley, Reading MA, 1989).
[39] C. W. J. Beenakker, Rev. Mod. Phys. **69**, 731 (1997).
[40] M. Duckheim and P. W. Brouwer, Phys. Rev. B **83**, 054513 (2011).
[41] See Supplemental Material at [].
[42] L. P. Gor'kov and E. I. Rashba, Phys. Rev. Lett. **87**, 037004 (2001).
[43] Y. Mizuno, T. Yokoyama, and Y. Tanaka, Phys. Rev. B **80**, 195307 (2009).
[44] J. Linder and T. Yokoyama, Phys. Rev. Lett. **106**, 237201 (2011).
[45] F. Dolcini and L. Dell'Anna, Phys. Rev. B **78**, 024518 (2008).
[46] K. Sun and N. Shah, Phys. Rev. B **91**, 144508 (2015).
[47] A. V. Balatsky, I. Vekhter, and J.-X. Zhu, Rev. Mod. Phys. **78**, 373 (2006).
[48] S. Wu and K. V. Samokhin, Phys. Rev. B **80**, 014516

(2009); **81**, 214506 (2010).
[49] M. Wimmer, M. Lobenhofer, J. Moser, A. Matos-Abiague, D. Schuh, W. Wegscheider, J. Fabian, K. Richter, and D. Weiss, Phys. Rev. B **80**, 161201 (2009).
[50] C. Betthausen, T. Dollinger, H. Saarikoski, V. Kolkovsky, G. Karczewski, T. Wojtowicz, K. Richter, and D. Weiss, Science **337**, 324 (2012).
[51] Z. Y. Chen, A. Biswas, I. Zutic, T. Wu, S. B. Ogale, R. L. Greene, and T. Venkatesan, Phys. Rev. B **63**, 212508 (2001).
[52] J. Alicea, Rep. Prog. Phys. **75**, 076501 (2012).